Microwave photonics with Josephson junction arrays

David Zueco,[1,2] Juan José Mazo,[1] Enrique Solano,[3,4] and Juan José García-Ripoll[5]

[1]Instituto de Ciencia de Materiales de Aragón y Departamento de Física de la Materia Condensada, CSIC-Universidad de Zaragoza, E-50012 Zaragoza, Spain.

[2]Fundación ARAID, Paseo María Agustín 36, 50004 Zaragoza, Spain

[3]Departamento de Química Física, Universidad del País Vasco Euskal Herriko Unibertsitatea, Apdo. 644, 48080 Bilbao, Spain

[4]IKERBASQUE, Basque Foundation for Science, Alameda Urquijo 36, 48011 Bilbao, Spain

[5]Instituto de Física Fundamental, IFF-CSIC, Serrano 113-bis, 28006 Madrid, Spain

(Dated: October 7, 2011)

We introduce an architecture for a photonic crystal in the microwave regime based on superconducting transmission lines interrupted by Josephson junctions. A study of the scattering properties of a single junction in the line shows that the junction behaves as a perfect mirror when the photon frequency matches the Josephson plasma frequency. We generalize our calculations to periodic arrangements of junctions, demonstrating that they can be used for tunable band engineering, forming what we call a *quantum circuit crystal*. As a relevant application, we discuss the creation of stationary entanglement between two superconducting qubits interacting through a disordered media.

PACS numbers: 42.50.Dv, 03.65.Yz, 03.67.Lx,

Circuit QED [1] is quantum optics on a superconducting chip: a solid state analogue of cavity QED in which superconducting resonators and qubits act as optical cavities and artificial atoms. After successfully reproducing many key experiments from the visible regime —qubit-photon strong coupling and Rabi oscillations [2], Wigner function reconstruction [3], cavity-mediated qubit-qubit coupling [4], quantum algorithms [5] or Bell inequalities measurement [6]—, and improving the quality factors of qubits and cavities, c-QED establishes as an alternative to standard quantum optical setups.

The next challenge in the field is the development of *quantum microwave photonics*. The scope is the generation, control and measurement of propagating photons, contemplating all its possibilities as carriers of quantum information and mediators of long distance correlations. The natural framework is that of active and passive *quantum metamaterials*, with open transmission lines to support propagation of photons, and embedded circuits to control them. Qubits could be a possible ingredient in these metamaterials. A two-level system may act as a saturable mirror for resonant photons [7], as it has been demonstrated in a breakthrough experiment with flux qubits [8], continued by further demonstrations of single photon transistors [9], and electromagnetically induced transparency [10]. These groundbreaking developments, together with theoretical studies of band engineering [7] and photodetection [11], provide solid foundations for this rapidly growing field.

In this work, we advocate an alternative route for developing passive quantum metamaterials. We introduce the idea of building *structured* transmission lines for the intrinsic control of propagating photons, *i.e.* band engineering. Our setup consists on microwave networks which are interrupted by the simplest and most fundamental device in superconducting technologies: the Josephson junction (JJ). Ordered and disordered arrays of JJs will act as elementary scatterers of photons, forming *quantum circuit crystals* where the propagation of photons can be controlled via band engineering. Finally we discuss the interaction of these quantum crystals with superconducting qubits. As a very relevant application we will demonstrate the potential of disordered quantum crystals as mediators of entanglement, and their connections with transport theory and nonlinear media.

Josephson junction as a scatterer.– JJs are the most versatile nonlinear element in circuit QED. Either alone, or in connection with extra capacitors or junctions, they form all types of superconducting qubits to-day [12]. Moreover, in recent years they have also been used inside cavities to shape and control confined photons, dynamically tuning the mode structure [13], enhancing the light-matter coupling [14, 15], or exploiting their nonlinearity in resonators [16]. In opposition to these closed setups, we also find JJs in open arrays where a variety of nonlinear phenomena and transport properties were studied [17, 18], but without individual photon resolution. In the following we will combine both approaches, providing a uniform theoretical framework to study the interaction of one or more junctions with propagating photons in an open line.

Our treatment is largely inspired by the studies of single photon scattering by superconducting qubits [7, 8]. We expect that arbitrary linear or nonlinear resonators (the JJs) may act as perfect scatterers of propagating photons, where in this case the *resonance* is determined by the JJ plasma frequency. Our setup is shown in Fig. 1, where the JJ plays the role of a localized scatterer interacting with incoming and outgoing wavepackets. The Lagragian for this system combines the one-dimensional field theory for a transmission line with the capacitivelyshunted-junction model for the junction [14, 16, 19]

$$\mathcal{L} = \frac{1}{2}\int_{-\infty}^{0_-} \mathrm{d}x \left[c_0 \dot{\phi}(x,t)^2 - \frac{1}{l_0}\partial_x \phi(x,t)^2 \right] \tag{1}$$
$$+ \frac{1}{2} C_J \delta\dot{\phi}^2 - I_C \cos\left(\frac{2\pi}{\Phi_0}\delta\phi\right)$$
$$+ \frac{1}{2}\int_{0_+}^{\infty} \mathrm{d}x \left[c_0 \dot{\phi}(x,t)^2 - \frac{1}{l_0}\partial_x \phi(x,t)^2 \right].$$

The field $\phi(x,t)$ represents flux on the line, whose capacitance and inductance per unit length, c_0 and l_0, we assume to be uniform just for simplicity (See Ref. [19] for generalizations). The junction, placed at $x = 0$, is characterized by a capacitance C_J and a critical current I_C, and governs the dynamics of the flux difference $\delta\phi = \phi(0^+) - \phi(0^-)$. Since we work in the few photon regime, we may linearize $\cos(2\pi\delta\phi/\Phi_0) \cong 1 - (2\pi\delta\phi/\Phi_0)^2$ replacing the JJ with an effective local oscillator characterized by its Josephson plasma frequency, $\omega_p = \sqrt{2\pi I_C/\Phi_0 C_J}$.

All stationary solutions of the previous model are linear combinations of incoming, reflected (r) and transmitted (t) plane waves, in the following form

$$\phi(x,t) = A_\phi \begin{cases} \mathrm{e}^{i(kx-\omega t)} + r\mathrm{e}^{-i(kx+\omega t)} & (x<0) \\ t\mathrm{e}^{i(kx-\omega t)} & (x>0) \end{cases} \tag{2}$$

where A_ϕ is some arbitrary field amplitude and the waves follow a linear dispersion relation, $\omega = vk$. The reflection and transmission coefficients are found by imposing that the intensities $I_{\text{left}} = \partial_x\phi(0^-,t)/l_0$, $I_{\text{junction}} = C_J\delta\ddot{\phi} + I_J \sin(2\pi\delta\phi/\Phi_0)$ and $I_{\text{right}} = \partial_x\phi(0^+,t)/l_0$ be equal at $x = 0$. For the explicit ansatz (2) this becomes

$$r = \frac{1}{1 + i2\frac{Z_0}{Z_J}\frac{1}{\bar{\omega}}\left(\bar{\omega}^2 - 1\right)}, \quad t = 1 - r, \tag{3}$$

with the rescaled photon frequency, $\bar{\omega} = \omega/\omega_p$, and the impedances of the line and the junction, $Z_J = \sqrt{L_J/C_J}$ with $L_J = \Phi_0/2\pi I_C$ and $Z_0 = \sqrt{l_0/c_0}$. This formula, which is analogous to the one for a qubit [7, 8], exhibits perfect reflection when the photon is on resonance with the junction, $\omega = \omega_p$, accompanied by the usual phase jump across it (cf. Fig. 1).

Quantum circuit crystals.– This quantum metamaterial consists of one or multiple microwave guides interrupted by a periodic arrangement of JJs. We conceive it as a generalization of photonic crystals to the quantum microwave regime, with similar capabilities for controlling the propagation of photons: engineered dispersion relations, gaps of forbidden frequencies, localized modes, adjustable group velocities and index of refraction, and control of the emission and absorption of embedded artificial atoms (i.e. improved cavities) [20].

The simplest possible instance of a quantum circuit crystal consists of a unit cell with N junctions that repeats periodically. In such case, the eigensolutions are

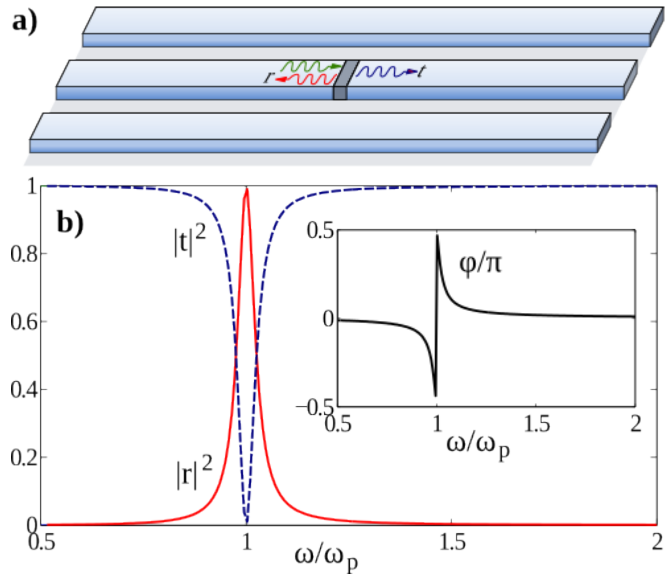

FIG. 1. (a) An open transmission line interrupted by a Josephson junction. (b) Reflection, r, transmission, t, and phase of the transmitted beam, $\varphi = \arg t$, vs. incoming photon frequency, in units of the plasma frequency ω_p. We use $Z_J = 10$.

translationally invariant and determined by the transfer matrix of the unit cell, T_{cell}, relating the field at both sides, $\phi_{L,R}(x) = a_{L,R}e^{ikx} + b_{L,R}e^{-ikx}$, through

$$\begin{pmatrix} a_R \\ b_R \end{pmatrix} = T_{\text{cell}}(\omega) \begin{pmatrix} a_L \\ b_L \end{pmatrix}. \tag{4}$$

For a setup with junctions and free lines, the transfer matrix has the form $T_{\text{cell}} = \prod_{i=1}^{N} T_i D_i$, where T_i is the transfer matrix of the i-th junction and D_i is the free propagator through a distance d_i

$$T_i = \begin{pmatrix} 1/t_i^* & -r_i^*/t_i^* \\ -r_i/t_i & 1/t_i \end{pmatrix},\ D_i = \begin{pmatrix} e^{i\omega d_i/v} & 0 \\ 0 & e^{-i\omega d_i/v} \end{pmatrix}. \tag{5}$$

The stationary states are given by $\det[T_{\text{cell}}(\omega) - e^{ip}] = 0$ or $2\cos(p) = \mathrm{Tr}[\hat{T}_{\text{cell}}(\omega)]$, where p is the quasimomentum of the Bloch wave in this structure.

As an example, Fig. 2 shows the dispersion relation $\omega(k)$ for the two simplest arrangements. The first one is a line with identical Josephson frequency ω_p and impedance Z_J, evenly spaced a distance d (cf. Fig. 2a). The second one is also periodic, but the unit cell contains two junctions with different properties, (ω_p, Z_J) and (ω_p', Z_J'), which are spread with two different spacings (cf. Fig. 2c). The consequence is that, in addition to the usual gap around the edge of the Brillouin zone, we find one band gap around $\omega = \omega_p$ in the first setup, and two band gaps around $\omega = \omega_p$ and $\omega = \omega_p'$ in the second, more complex case.

Microwave photonic crystals have a variety of applications [20]. The first one is the suppression of spontaneous emission from qubits, which is achieved tuning

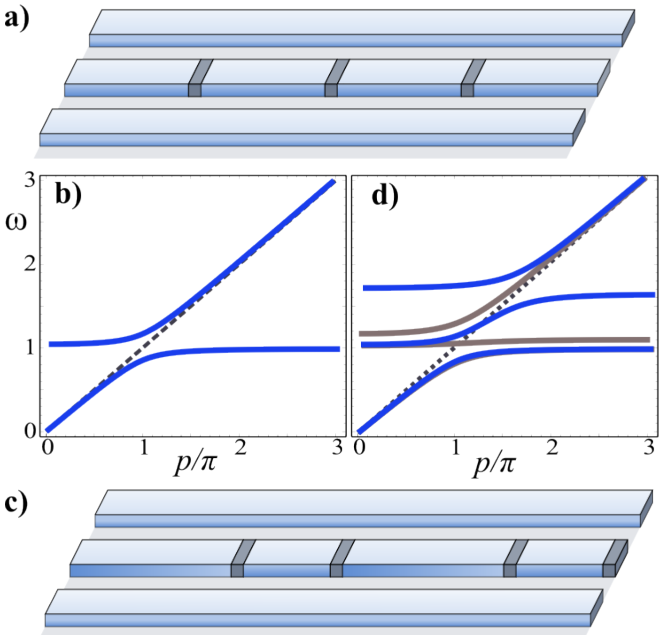

FIG. 2. Photonic crystals with one (a) or two (c) junctions per unit cell and their respective energy bands (b and d) vs. quasimomentum p. We use $Z_J = 10$. In (d) $\omega_p'/\omega_p = 0.6$ (blue) or 0.9 (gray) and and the distance inside the unit cell is $0.01/d$. Notice in (d) that in the lower band the gray and blue line are indistinguishable.

their frequency to lay exactly in the middle of a band gap. Another application is the dynamical control of group velocities. While the width of the band gaps is more directly related to the values of Z_J and the separation among scatterers, their position depends on the scatterer frequency, ω_p. Replacing the JJs with SQUIDS, it becomes possible to dynamically tune those frequencies and the slopes of the energy bands, changing from large group velocities (large slope) to almost flat bands (cf. Fig. 2d) where photons may be effectively frozen. Flat bands may be used to create quantum memories, but also to induce a tight-binding model on the photons, in the spirit of coupled-cavity systems [21, 22]. A third application is the engineering of dissipation where photonic crystals provide a new arena for theoretical and experimental studies. We will focus on this point, studying the relation between disorder, localization and entanglement generation in 1D *quantum circuit crystals*.

Entanglement through disorder.– It is feasible to produce regular circuit photonic crystals where, despite fabrication errors, the junctions within the same sample are very similar. Nevertheless it can be interesting to induce noise in the scattering elements, either statically, intervening in the design or deposition processes, or dynamically, replacing the junctions with SQUIDs and dynamically tuning their frequencies. Noise may have a dramatic influence in the transport properties of the photonic crystal [23]. On the one hand, the transmission coefficient averaged over an ensemble of random scatterers $\langle T\rangle$ decays exponentially with increasing length L of the disordered media, similar to Anderson's localization [24]. On the other hand, noise fights against the interference phenomena that gives rise to the existence of band gaps. The consequence of this competition will be that a sufficiently large noise could restore the transmission in the frequency range that was originally forbidden [23, 25, 26]. In what follows we exploit this phenomenon in connection to a purely quantum effect: the entanglement generation through disordered media.

Our model setup consists on two well separated flux qubits which are coupled by a quantum circuit random crystal [Fig. 3]. The qubits will be at their degeneracy points and one of them suffers an external resonant driving $\omega_{\rm d} = \epsilon$, $H_{\rm q} = \frac{\epsilon}{2}(\sigma_1^z+\sigma_2^z)+f(\mathrm{e}^{-i\omega_{\rm d}t}\sigma_1^+ + \text{H.c.})$. In addition to this, the qubit dynamics is influenced by the coupling to a μwave line that has been interrupted by a set of JJ forming a disordered crystal. We model the qubit-line coupling through the spin boson Hamiltonian [7, 9], while the line itself follows our previous scattering theory with uniform noise δ in the frequency $\omega_p \to \omega_p^{(0)}(1+\delta)$ and impedance $Z_J \to Z_J^{(0)}(1+\delta)$. Tracing out the transmission line one ends up with a master equation for the two qubit reduced density matrix [27, 28]

$$\frac{\partial \varrho}{\partial t} = -i[\widetilde{H}_{\rm q} + H_{\rm LS}, \varrho] - \sum_{i,j=1}^{2} \gamma_{ij}\left([\sigma_i^+, \sigma_j^- \varrho] + \text{H.c.}\right). \quad (6)$$

Here, $\tilde{H}_{\rm q}$ is the qubit Hamiltonian in the interaction picture and $H_{\rm LS} = J_{12}(\sigma_1^+\sigma_2^- + \sigma_1^-\sigma_2^+)$. Notice how the qubits are coupled coherently, through vacuum fluctuations or *Lamb shift*, $J_{12} = \gamma_0 \mathrm{Im}(T\exp(-ik2D))/2$, and also incoherently, through the cross-dissipation rate $\gamma_{12} = \gamma_0 \mathrm{Re}(T\exp(-ik2D))$. These interactions compete with the individual decay rates of the qubits, $\gamma_{ii} = \gamma_0(1-\mathrm{Re}(R\exp(-ikD))) + \lambda$, which includes a phenomenological non-radiative decay channel, λ. In all these formulas appear the effective rate $\gamma_0 = \pi\hbar^2 g^2/vk$, the total transmission and reflection through the line, T and R, and the qubit-crystal separation, D, which in our simulations disappears, as we will maximize over D.

The physical picture that results is intuitively appealing: for the qubits to be entangled, the noisy environment should be able to transmit photons, $T \neq 0$, as both the coherent and incoherent couplings depend on it. Moreover, all photons which are not transmitted but reflected add up to the ordinary spontaneous emission rates of the qubits, γ_{ii}. And finally, for a wide parameter range the two qubits are entangled also at $t\to\infty$, in the stationary state of the combined system, $\partial_t \varrho_{\rm stationary} = 0$. We have quantified the asymptotic amount of entanglement using the concurrence, C, for a variety of noise intensities in a medium which is composed of $N = 20$ junctions which are uniformly spread over a distance $L = 2\lambda$. Fig. 3

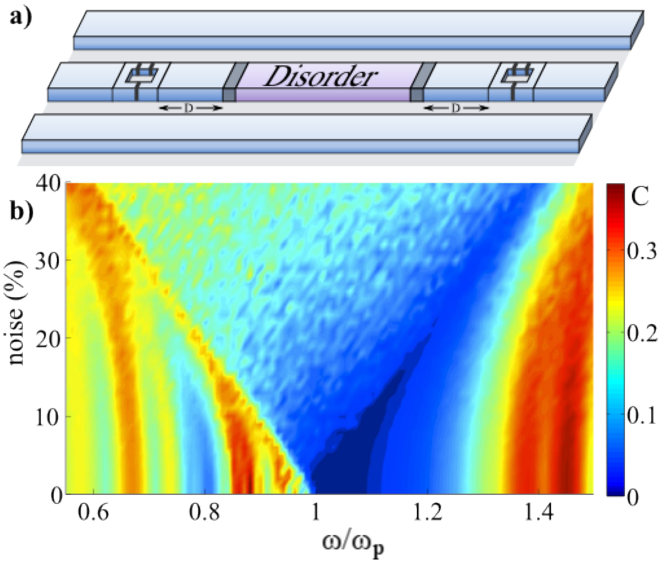

FIG. 3. (a) Two qubits connected by a noisy environment. (b) Concurrence between the qubits for model (6) as a function of frequency and fabrication error (δ). We simulated a setup with 20 junctions regularly spaced over a distance $L = 2\lambda$, averaging over 500 realizations. We use the parameters, $Z_J = 10$, $\epsilon = \omega_d$, $\lambda = 0.4\gamma_0$ and $f = 0.1\gamma_0$.

shows the result of averaging 500 realizations of disorder and contains the two ingredients stated above. We observe that for zero or little disorder entanglement becomes zero at the band gap, $\omega/\omega_p = 1$, where photons are forbidden due to interference. However, as we increase disorder the gap vanishes and entanglement enters the region around it. Outside the gap the effect is the opposite: disorder reduces the amount of entanglement, as it hinders the transmission of photons. To understand the modulations of the plot one must simply realize that the value of C mostly depends on the ratio between γ_{12} and γ_{ii}, and these are complex functions of T and R, respectively [28, 29].

Summing up, in this work we have introduced the notion of quantum circuit crystal, a superconducting circuit formed by periodic arrangements of Josephson junctions along a microwave transmission line. Closely related to the JJ arrays, these metamaterials can be used to control the propagation of individual photons and their interaction with stationary qubits. We combine both in a setup with noisy quantum circuit crystals, where noise and dissipation ally to generate stationary entanglement among distant qubits. This type of entanglement is robust and will survive moderate amounts of dephasing and other errors in the setup. As further applications we envision the extension of these ideas to two-dimensional and fractal arrangements, with the aim of engineering actual wavefronts and negative index of refractions, as well as the engineering of photon-photon interactions and nonlinearities in these artificial media.

We acknowledge Frank Deppe, Carlos Fernández-Juez and Luis Martín-Moreno for discussions. This work was supported by Spanish MICINN projects FIS2008-01240, FIS2009-10061 and FIS2009-12773-C02-01 cofinanced by FEDER funds. CAM research consortium QUITEMAD, Basque Government IT472-10, SOLID and CCQED European projects.

[1] J. Q. You and F. Nori, Nature (London) **474**, 589 (2011).
[2] A. Wallraff, D. I. Schuster, A. Blais, L. Frunzio, R.-S. Huang, J. Majer, S. Kumar, S. M. Girvin, and R. J. Schoelkopf, Nature **431**, 162 (2004).
[3] M. Hofheinz, H. Wang, M. Ansmann, R. C. Bialczak, E. Lucero, M. Neeley, A. D. O'Connell, D. Sank, J. Wenner, J. M. Martinis, and A. N. Cleland, Nature **459**, 546 (2009).
[4] J. Majer, J. M. Chow, J. M. Gambetta, J. Koch, B. R. Johnson, J. A. Schreier, L. Frunzio, D. I. Schuster, A. A. Houck, A. Wallraff, A. Blais, M. H. Devoret, S. M. Girvin, and R. J. Schoelkopf, Nature (London) **449**, 443 (2007).
[5] L. Dicarlo, J. M. Chow, J. M. Gambetta, L. S. Bishop, B. R. Johnson, D. I. Schuster, J. Majer, A. Blais, L. Frunzio, S. M. Girvin, and R. J. Schoelkopf, Nature **460**, 240 (2009).
[6] M. Ansmann, H. Wang, R. C. Bialczak, M. Hofheinz, E. Lucero, M. Neeley, A. D. O'Connell, D. Sank, M. Weides, J. Wenner, A. N. Cleland, and J. M. Martinis, Nature **461**, 504 (2009).
[7] J.-T. Shen and S. Fan, Phys. Rev. Lett. **95**, 213001 (2005).
[8] O. Astafiev, A. M. Zagoskin, A. A. Abdumalikov, Y. Pashkin, T. Yamamoto, K. Inomata, Y. Nakamura, and J. S. Tsai, Science **327**, 840 (2010).
[9] I.-C. Hoi, C. M. Wilson, G. Johansson, T. Palomaki, B. Peropadre, and P. Delsing, Phys. Rev. Lett. **107**, 073601 (2011).
[10] O. V. Astafiev, A. A. Abdumalikov, A. M. Zagoskin, Yu, Y. Nakamura, and J. S. Tsai, Phys. Rev. Lett. **104**, 183603 (2010).
[11] G. Romero, J. J. García-Ripoll, and E. Solano, Phys. Rev. Lett. **102**, 173602 (2009).
[12] Y. Makhlin, G. Schön, and A. Shnirman, Rev. Mod. Phys. **73**, 357 (2001).
[13] C. M. Wilson, G. Johansson, A. Pourkabirian, J. R. Johansson, T. Duty, F. Nori, and P. Delsing, ArXiv e-prints (2011), arXiv:1105.4714 [quant-ph].
[14] T. Niemczyk, F. Deppe, H. Huebl, E. P. Menzel, F. Hocke, M. J. Schwarz, J. J. Garcia-Ripoll, D. Zueco, T. Hummer, E. Solano, A. Marx, and R. Gross, Nature Physics **6**, 772 (2010).
[15] P. Forn-Díaz, J. Lisenfeld, D. Marcos, J. J. García-Ripoll, E. Solano, C. J. P. M. Harmans, and J. E. Mooij, Phys. Rev. Lett. **105**, 237001 (2010).
[16] F. R. Ong, M. Boissonneault, F. Mallet, A. Palacios-Laloy, A. Dewes, A. C. Doherty, A. Blais, P. Bertet, D. Vion, and D. Esteve, Phys. Rev. Lett. **106**, 167002 (2011).
[17] R. Newrock, C. Lobb, U. Geigenmüller, and M. Octavio, *The Two-Dimensional Physics of Josephson Junction Arrays*, Solid State Physics, Vol. 54 (Academic Press, 1999)

pp. 263 – 512.
[18] J. J. Mazo and T. P. Orlando, Chaos **13**, 733 (2003).
[19] J. Bourassa, J. M. Gambetta, A. A. Abdumalikov, O. Astafiev, Y. Nakamura, and A. Blais, Phys. Rev. A **80**, 032109 (2009).
[20] J. Joannopoulos, S. Johnson, J. Winn, and R. Meade, *Photonic Crystals: Molding the Flow of Light*, 2nd ed. (Princenton, 2008).
[21] M. J. Hartmann, F. G. S. L. Brandão, and M. B. Plenio, Nature Physics **2**, 849 (2006).
[22] D. G. Angelakis, M. F. Santos, and S. Bose, Phys. Rev. A **76**, 031805 (2007).
[23] M. A. Kaliteevski, D. M. Beggs, S. Brand, R. A. Abram, and V. V. Nikolaev, Phys. Rev. B **73**, 033106+ (2006).
[24] M. V. Berry and S. Klein, Eur. J. Phys. **18**, 222 (1997).
[25] S. John, Phys. Rev. Lett. **58**, 2486 (1987).
[26] Yu, M. A. Kaliteevski, and V. V. Nikolaev, Phys. Rev. B **60**, 1555 (1999).
[27] A. Gonzalez-Tudela, D. Martín-Cano, E. Moreno, L. Martín-Moreno, C. Tejedor, and F. J. García-Vidal, Phys. Rev. Lett. **106**, 020501 (2011).
[28] See EPAPS.
[29] Y. Chang, Z. R. Gong, and C. P. Sun, Phys. Rev. A **83**, 013825 (2011).

SUPPLEMENTARY MATERIAL

Modelling qubit-line interaction

In this section we model the qubit-line interaction. Here, we consider flux qubits but other superconducting qubit architectures are analogous.

For flux qubits the coupling is inductive and can be written in “circuit language” and/or “magnetic language” as,

$$H_{\text{int}} = M I_{\text{qubit}} \times I_{\text{line}} = \mu B \ , \tag{7}$$

here M stands for the mutual inductance, I_{qubit} and I_{line} are the currents and μ is the magnetic qubit dipole, while B is the magnetic field generated in the cavity. The current in the line is given by

$$I_{\text{line}} = \frac{1}{l_0}\partial_x \phi(x) \tag{8}$$

and ϕ is the flux.

The normal mode quantization starts by expanding, $\phi(x,t) = \int \mathrm{d}k u_k(x) q_k(t)$. We choose to have u_k dimensionless. Therefore the u_n satisfy the orthonormality condition,

$$\int \mathrm{d}x c_0 u_k \ u_l = C_r \delta_{kl} \ , \qquad\qquad C_r := \int \mathrm{d}x c_0 \tag{9}$$

with $u_n(x)$ the normal modes. Then the time dependent amplitudes are quantized,

$$q_n = \sqrt{\frac{\hbar}{2\omega_n C_r}}(a_n^\dagger + a_n) \tag{10}$$

giving the expression for the current:

$$I_{\text{line}} = \frac{1}{l_0}\int \mathrm{d}k \sqrt{\frac{\hbar}{2\omega_k C_r}}\partial_x u_k(x)(a_k^\dagger + a_k) \ . \tag{11}$$

On the other hand, the magnetic field-current relation is given by:

$$B_{\text{line}} = \frac{\mu_0 I_{\text{line}}}{\pi d} \tag{12}$$

with d the distance between plates in the coplanar wave-guide. Finally, the quantized magnetic dipole for the qubit is,

$$\mu = I_p A \sigma^x \tag{13}$$

with A the area loop. Putting alltogether we find that the interaction Hamiltonian (7) can be written as,

$$H_{\text{int}} = I_p A \times \frac{\mu_0}{\pi d} \times \frac{1}{l_0} \times \frac{\hbar}{2C_r}\sigma_x \otimes \int \mathrm{d}k \frac{1}{\sqrt{\omega_k}} \partial_x u_k(x)(a_k^\dagger + a_k) \ . \tag{14}$$

We can introduce the coupling strenght per mode with frequency ω_0 [1],

$$\hbar g = I_p A \frac{\mu_0}{\pi^{3/2} d} \omega_0 \sqrt{\frac{1}{\hbar Z_0}} \tag{15}$$

Grouping the constants and using the expression for g, Eq. (15), we rewrite (14),

$$H_{\rm int} = \hbar \frac{g}{\omega_0} v^{3/2} \frac{\pi}{\sqrt{2L}} \sigma_x \int {\rm d}k \frac{1}{\sqrt{\omega_k}} \partial_x u_k(x) (a_k^\dagger + a_k) \tag{16}$$

where $v = 1/\sqrt{l_0 c_0}$ the light velocity in the line and ω_0 the fundamental frequency of a cavity with a given g and L is the Lenght. As expected the above is nothing but the spin boson model.

Quantum Master Equation for the qubits placed in the line

We discuss the master equation governing the dynamics of two independent flux qubits coupled to the line. Using the results of the previous section we write (16) as,

$$H_{\rm int} = \sum_{j=1,2} \sigma_j^x \otimes \int {\rm d}k X_k(x_j) \tag{17}$$

here x_j stands for the points where the qubits are, and $X_k(_j)$ reads,

$$X_k(x_j) = \hbar \frac{g}{\omega_0} v^{3/2} \frac{\pi}{\sqrt{2L}} \frac{1}{\sqrt{\omega_k}} \partial_x u_k(x_j) (a_k^\dagger + a_k) \tag{18}$$

The other terms in the Hamiltonian are the line and qubits ones,

$$H_{\rm line} = \int {\rm d}k \omega_k a_k^\dagger a_k \qquad H_{\rm qubits} = \frac{\omega_{\rm qubit}}{2} \sum_{j=1,2} \sigma_j^z \,. \tag{19}$$

yielding the total Hamiltonian,

$$H_{\rm total} = H_{\rm qubits} + H_{\rm line} + H_{\rm int} \,. \tag{20}$$

Assuming temperature zero (typical experiments are at the mK while frequencies are GHz) the qubit dynamics, after integrating the bosonic modes, is given by the *standard* master equation in Linblad form, [2],

$$\partial_t \rho = -\frac{i}{\hbar} [H_{\rm qubit} + H_{\rm LS}, \rho] + \sum_{j,j'} \Gamma_{j,j'} \left(\sigma_j^- \rho \sigma_{j'}^+ - \frac{1}{2} \{ \sigma_j^+ \sigma_{j'}^- \rho \} \right) + \lambda \sum_{j,j'} \left(\sigma_j^- \rho \sigma_j^+ - \frac{1}{2} \{ \sigma_j^+ \sigma_j^- \rho \} \right) \tag{21}$$

where $\{,\}$ is the anticonmutator. In the equation we have splitted the decays contributions due to the qubit-line coupling and to other noise sources affecting the qubits with a phenomenological strenght λ. The explicit expressions for $\Gamma_{j,j'}$ are,

$$\Gamma_{j,j'} = \pi^2 \left(\frac{g}{\omega_{\rm qubit}} \right)^2 \frac{v^3}{L} \int {\rm d}k \partial_x u_k(x_j) \partial_x u_k(x_{j'}) \delta(\omega_k - \omega_{\rm qubit}) \tag{22}$$

and $H_{\rm LS}$ is the *Lamb Shift*:

$$H_{\rm LS} = \Delta_{12} \left(\sigma_1^+ \sigma_2^- + \sigma_2^+ \sigma_1^- \right) \tag{23}$$

with,

$$\Delta_{12} = \frac{\pi}{2} \left(\frac{\hbar g}{\omega_{\rm qubit}} \right)^2 \frac{v^3}{L} \mathcal{P} \left[\int {\rm d}k \frac{1}{\omega_k} \frac{\partial_x u_k(x_1) \partial_x u_k(x_1)}{\omega_{\rm qubit} - \omega_k} \right] \tag{24}$$

where $\mathcal{P}[\,]$ means principal value integral.

Master Equation and the Green Function in the line

It turns out useful to rewrite the above master equation, in terms of the Green Function for the line. The idea is to relate the photonic transport properties with both the coherent coupling in $H_{\rm LS}$ and the cross-dissipation rates Γ_{jk}. We begin the discussion recalling the wave equation for the field in the line. Equivalently to layered photonic crystals, it is sufficient to work the case of homogeneous line, since the problem we are dealing with is piecewise homogeneous[3]. Being definite,

$$\frac{1}{l_0}\partial_x^2\phi = c_0\ddot{\phi} \tag{25}$$

the idea is to find the eigenvalues of this Sturm-Lioville problem, by expanding in normal modes $\phi = \sum_n q_n(t)u_n(x)$,

$$\frac{1}{l_0}\partial_x^2 u_n = -\omega_k^2 c_0 u_k \tag{26}$$

For flux qubits the coupling is via the current in line [cf. Eq. (8)]. Thus, it is convenient to discuss the expansion in terms of their derivatives, rather that in terms of u_n. The equation is the same,

$$\frac{1}{l_0}\partial_x^2(\partial_x u_k) = -\omega_n^2 c_0 \partial_x u_k \tag{27}$$

but with the orthogonality condition,

$$\int \mathrm{d}x \partial_x u_k \partial_x u_{k'} = L k^2 \delta_{kk'} \tag{28}$$

The Green function for this partial diferential equation reads,

$$\partial_x^2 G(x,x',\omega) + \frac{\omega^2}{v^2}G(x,x',\omega) = -\delta(x-x') \tag{29}$$

It is pivotal the relation [cf. Eq. (8.114) in [3]]

$$\mathrm{Im}G(x,x',\omega) = \frac{v^4}{L}\frac{\pi}{2}\sum_k \frac{\partial_x u_k(x)\partial_x u_k^*(x')}{\omega_k^3}\delta(\omega-\omega_k) \tag{30}$$

Replacing the above (30) in the expressions for $\Gamma_{jj'}$, Eq. (22) and Δ_{12}, Eq. (24) we obtain:

$$\Gamma_{jk}(\omega_{\rm qubit}) = 2\pi\frac{(\hbar g)^2}{v}\mathrm{Im}G(r_j, r_k, \omega_{\rm qbuit}) \tag{31}$$

and,

$$\Delta_{jk} = \frac{(\hbar g)^2}{v}\frac{1}{\omega_{\rm qubit}}\mathcal{P}\left[\int \mathrm{d}\omega \frac{\omega^2 \mathrm{Im}G(r_j, r_k, \omega_{\rm qbuit})}{\omega_{\rm qubit}-\omega}\right] \tag{32}$$

Green Function

In the following we find $G(r_j, r_{j'}, \omega)$ for the problem discussed in the main text. We show that $G(r_i, r_j, \omega)$ is written in terms of reflection and transmission coefficients, R and T respectively. As a consequence, we will rewrite the expressions for the decays and cross couplings, Γ_{ij} and Δ_{12}, Eqs. (31) and (32) in terms of the latter, making explicit the connection between the photonic transport in the line and the dynamics for the qubits coupled to it.

In our case, two qubits placed at possitions x_1 and x_2 with a set of junctions in between (see figure 4) $G(r_j, r_{j'}, \omega)$ can be computed as follows. T he equation for the Green function (29) is a field equation with a source (because of the Dirac delta) at $x = x'$. The junctions cover the region from $x = 0$ to $x = L$, therefore $x_1 < 0$ and $x_2 > L$. This situation is analogous to have a bounday with reflection R and transmission T, as despicted in figure 4). In this situation the Green Function is given by [Eqs. (2.34) and (2.35) in [4]],

$$G(x,x',\omega) = \begin{cases} \frac{i}{2k}\left(\mathrm{e}^{-ik(x-x')} - R\mathrm{e}^{-ik(x+x')}\right) & x < x' \\ \frac{i}{2k}\left(\mathrm{e}^{ik(x-x')} - R\mathrm{e}^{-ik(x+x')}\right) & x' < x < 0 \\ \frac{i}{2k}T\mathrm{e}^{ik(x-(x'+L))} & x > L \end{cases} \tag{33}$$

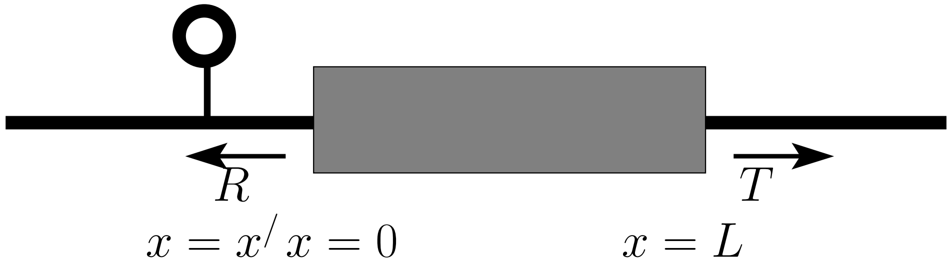

FIG. 4. Sketch for the Green function calculation. The “black box” is characterized by transmission and reflection coefficientes. The source (Dirac Delta) is represented by the ring attached to the line.

We remind that the minus sign in front of the R above comes because the Green function in (30) is given in terms of $\partial_x u_k$.

Finally, the coefficients in the master equation read [Cf. Eqs. (31) and (32)]

$$\Gamma_{jj}(\omega_{\rm qubit}) \quad = 2\pi\tfrac{(\hbar g)^2}{v}{\rm Im}G(r_j, r_j, \omega_{\rm qbuit}) = 2\pi\tfrac{(\hbar g)^2}{v}\tfrac{1}{2k}\Big(1 + {\rm Re}(R)\Big) \tag{34}$$

$$\Gamma_{12}(\omega_{\rm qubit}) = 2\pi\tfrac{(\hbar g)^2}{v}{\rm Im}G(r_1, r_2, \omega_{\rm qbuit}) = 2\pi\tfrac{(\hbar g)^2}{v}\tfrac{1}{2k}{\rm Re}(T{\rm e}^{-ik(x_1-x_2)}) \tag{35}$$

The last obstacle to write the master equation is to perform the integral in (32). Here we made use of the so called Generalized Kramers-Kroning relation [5], namely

$$\mathcal{P}\left[\int_0^\infty {\rm d}\omega\frac{\omega^2}{v^2}\frac{{\rm Im}G(r_j, r_k, \omega)}{\omega - \omega_{\rm qubit}}\right] = \frac{\pi}{2}\frac{\omega_{\rm qubit}^2}{v^2}{\rm Re}G(r_j, r_k, \omega) \tag{36}$$

Thus,

$$\Delta_{12} = \pi\frac{(\hbar g)^2}{v}\frac{1}{2k}{\rm Im}(T{\rm e}^{-ik(x_1-x_2)}) \tag{37}$$

Introducing the definition,

$$\gamma_0 = \pi\frac{(\hbar g)^2}{v}\frac{1}{k} \tag{38}$$

we end up with the expressions used in the main text.

Averaged Quantities

The quantities in disorder theory are averaged over different realization of the disorder. The averaged is defined as,

$$\bar{A} = \frac{1}{N_{\rm realizations}}\sum_{\rm realizations} A_i \tag{39}$$

where $N_{\rm realizations}$ is the number of realizations and A_i the result obtained in each of them.

[1] T. Lindström, C. H. Webster, J. E. Healey, M. S. Colclough, C. M. Muirhead, and A. Y. Tzalenchuk, Superconductor Science and Technology **20**, 814 (2007).
[2] H.-P. Breuer and F. Petruccione, *The Theory of Open Quantum Systems* (Oxford University Press, USA, 2007).
[3] L. Novotny and B. Hecht, *Principles of Nano-Optics* (Cambridge University Press, 2006).
[4] C.-T. Tai, *Dyadic Green Functions in Electromagnetic Theory (Ieee-Oup Series on Electromagnetic Wave Theory)*, 2nd ed. (Oxford University Press, USA, 1996).
[5] D. Dzsotjan, J. Kästel, and M. Fleischhauer, Phys. Rev. B **84**, 075419 (2011).